



Development of a Reconfigurable Thoracentesis Training Mannequin

Andre Khayat¹ , R. Jill Urbanic² , Anna Farias³  and Beth-Anne Schuelke-Leech⁴ 

¹University of Windsor, khayata@uwindsor.ca

²University of Windsor, jurbanic@uwindsor.ca

³University of Windsor, afarias@uwindsor.ca

⁴University of Windsor, Beth-Anne.Schuelke-Leech@uwindsor.ca

Corresponding author: R. Jill Urbanic, jurbanic@uwindsor.ca

ABSTRACT

Using conventional methodologies, the development of complex products such as a thoracentesis training mannequin may take months to achieve and may require a large initial investment for the manufacturing of the molds. Currently, training for thoracentesis uses inflexible, costly, or unrealistic models, largely in part due to the techniques and tools used to develop them. These models are proven to be effective for their respective demographics, but there is much room for improvement. The goal of this research is to develop a more representative model for thoracentesis training that is reconfigurable for different patient sizes and weights. To achieve this goal, scaling factors are determined for key human anatomy, and parametric relationships developed for manufacturing molds. Experimental procedures are performed to accurately emulate the tissues of the human body. This research shows the potential of creating flexible, reconfigurable products using advanced CAD and additive manufacturing techniques, to improve medical training.

Keywords: reconfigurable medical training mannequin, additive manufacturing, CAD.

DOI: <https://doi.org/10.14733/cadaps.2019.1127-1145>

1 INTRODUCTION

Product development is a critical component of engineering. Companies need to innovate in order to stay competitive. New design and manufacturing tools, techniques, and processes allow for the development of better products and services. Through the implementation of new manufacturing tools and techniques (particularly computer-aided design, computer-aided manufacturing, and additive manufacturing), more realistic and cost effective design and engineering solutions may be obtained. While conventional manufacturing methodologies (molding, welding, machining, etc.)

require extensive process knowledge and require significant capital investment for the machines, tooling, jigs and fixtures [[1]], new manufacturing tools and techniques allow complicated designs to be continuously and quickly updated and refined. Additionally, advanced materials can be incorporated into the design. Large capital and material costs are avoided, making the whole process much more inexpensive and flexible.

CAD models combined with additive manufacturing (AM) processes are providing new means to improve biomedical prototypes and products. Although existing solutions may be useful for 'general' situations, a customized solution may enhance a 'quality of life' condition, as complex patient-specific or demographic-specific designs can be readily fabricated with the AM or 3D printing processes. Because of the process flexibility associated with AM, significant growth in the medical domain is occurring, especially for knee, hip, and spinal implants [[42]], as well as prosthetics [[16]].

Process planning solutions are contingent on the product complexity (i.e., shape and number of components), production volumes and planning horizon. Conventional manufacturing methodologies require extensive process planning, have a large number of variables to be controlled, and a high degree of design and fabrication knowledge. In contrast, the process planning for AM processes correlate well to a laser printing process: a user selects a material, a build mode (i.e., draft), and a build orientation. There is a limited set of default settings, and the actual process parameters (material feed rate, system temperature controls, travel speed, etc.), are unknown, and irrelevant to a user unless an open source system is being used [[32]], or specific manufacturing traits are desired. AM solutions have reduced the process planning and fabrication complexity; however, prior to fabricating a product, manifold or 'watertight' CAD models must be created, and biomedical CAD models are challenging to create due to their shape complexity. One example of this is a thoracentesis training mannequin. Currently, training for this procedure uses unrealistic models, with incomplete palpation landmarks, as discussed in the next section.

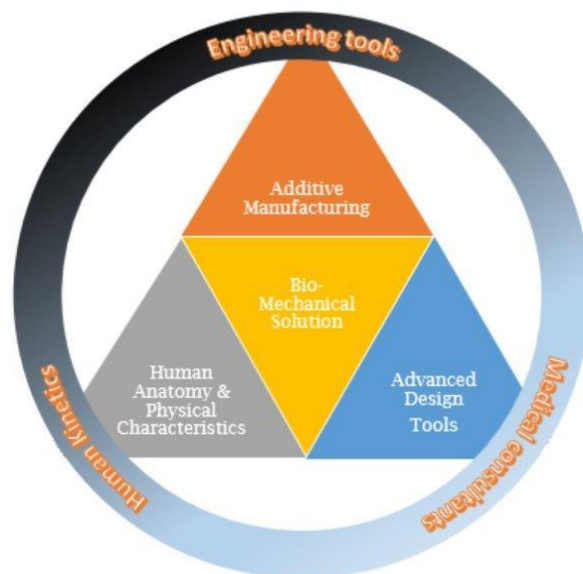


Figure 1: Multidisciplinary approach to bio-mechanical solutions.

The objective of this research was to investigate how these new manufacturing tools and processes can be systematically combined to improve the product development process. Specifically, the goal was to develop a more realistic and inexpensive medical training mannequin that is reconfigurable

for different patient sizes and weights. A cross-disciplinary approach was employed in the research (Figure 1), combining engineering tools and knowledge with medical and kinesiology expertise, to build a parametric (dynamic) model, which was used to build and test a prototype. Scaling factors were investigated to determine relationships for the key human anatomy models, for which parametric manufacturing molds were developed. Experiments were conducted to determine the desired resistance force profiles to guide the material selection and molding strategies. Using the parametric model and advanced manufacturing tools, a multi-step over-molding solution was developed to create realistic training model prototypes. This research shows the potential of creating flexible, reconfigurable products and processes, to improve medical training.

2 LITERATURE REVIEW

2.1 Introduction to the Thoracentesis Procedure and Training Mannequins

When the proper function of the lungs is impaired due to a pooling of fluid in the lungs, fluid has seeped into the pleural space. This is the space between the visceral and pleural membranes that surround the lungs within chest cavity (Figure 2). This condition is referred to as a pleural effusion [[36]] (Figure 2). Causes for a pleural effusion include: cancer, infections, pulmonary embolisms, heart failure, organ transplants and autoimmune conditions [[23]], [[31]], [[35]], [[36]] while shortness of breath, chest pain, and dizziness are common symptoms.

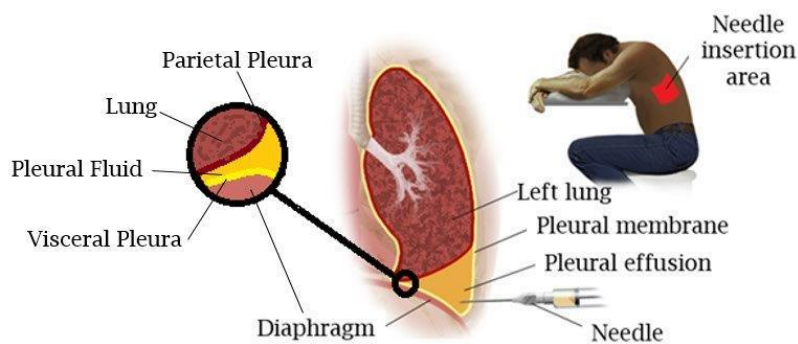


Figure 2: Pleural space and pleural effusion (adapted from [[28]]).

To drain this fluid, a thoracentesis is performed (Figure 3(a)). A wide bore needle is inserted through the chest wall, into the pleural space to drain the fluid (Figure 3(b)) [[19]]. The 18-20-gauge, 3.5 in. (89 mm) catheter/needle [[3]] is typically inserted normal to the skin approximately one inch (25 mm) deep, depending on chest wall thickness. The insertion location point and the duration of the procedure will vary depending on the amount of fluid to be drained, however the general site determination uses a palpation sequence consisting of the clavicle, the lower part of the scapula, and the rib cage "tracing".

Using conventional teaching methodologies (Figure 4), major complications associated with improper procedure such as lacerations of internal organs, bleeding, infection or pneumothorax (introduction of air into the pleural space), have occurred up to 11% of the time when performed by a professional [[6]]. In residents, these rates have been shown to increase up to 30% of the time, showing a correlation between experience and performance in thoracentesis procedure [13]. Ferrie et al. have stated that in their study, 40% of emergency physicians they tested were unable to identify key landmarks for an optimal puncture on test subjects [[9]].

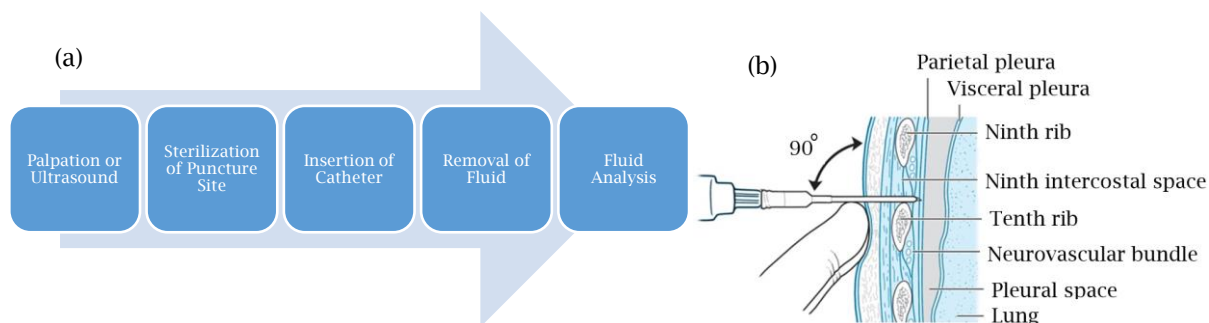


Figure 3: (a) Thoracentesis procedure, (b) Insertion of thoracentesis needle (adapted from [[30]]).



Figure 4: Conventional thoracentesis skill teaching methodology summary.

In order to improve on these observed findings, alternative educational means have been implemented. Training mannequins are gaining in popularity as they offer a hands-on learning experience without having to wait for patients willing to allow them to practice, and eliminate the anxiety detailed by Huang et al., who have stated that most Internal Medicine (IM) residents express feelings of increased discomfort with this procedure, especially given its invasive, and unnerving nature [[14]]. These mannequins have been proven to be effective in numerous studies, including one performed by Wayne et al., who showed the improvement in both written and clinical skills exams following a brief training session with a thoracentesis simulator (Figure 5(a)) [[40]], and another study by Guanchao et al., who explored the knowledge and clinical skill curves and retention of residents trained using simulator mannequins (Figure 5(b)) [[11]]. These positive results are slightly skewed, given that the training and testing were performed on the same mannequin, and that there was no variability in the landmark orientation or body composition, as discussed in section 2.2.

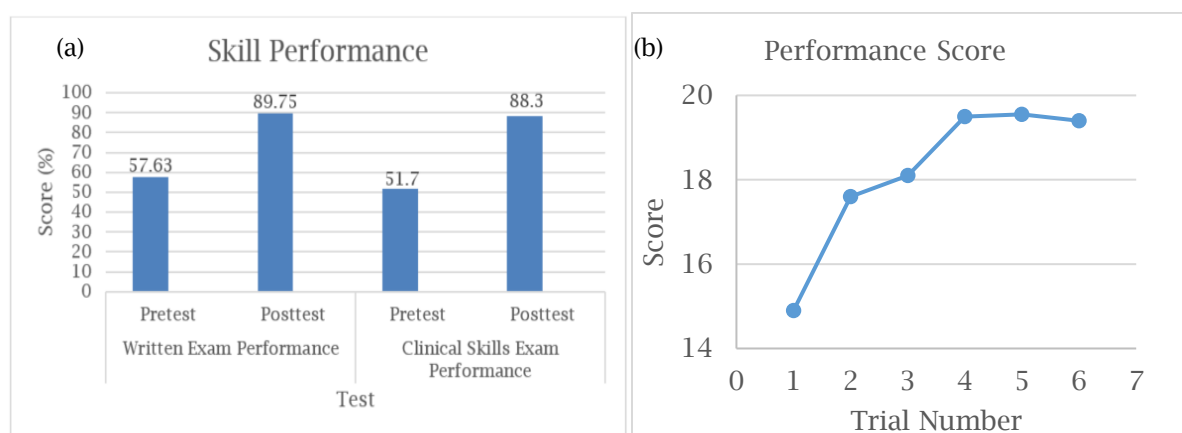


Figure 5: (a) Pre and post training test scores (adapted from Wayne et al. [[40]]), (b) Performance score learning curve with thoracentesis training mannequin (adapted from Guanchao et al. [[11]]).

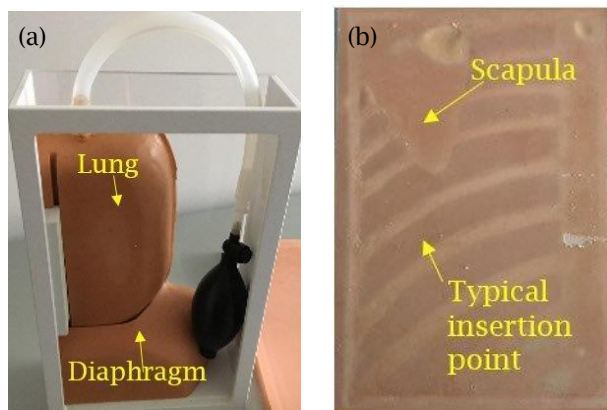


Figure 6: (a) Ultrasound thoracentesis model (THM-30) (Simulab Corporation [[37]]), (b) Flat rib cage “sheet” [[37]].

Existing thoracentesis training mannequin solutions are analyzed in terms of their strengths, weaknesses, and a selected set are summarized in Tab. 1. It can be seen that the mannequins are compact, portable, and provide fluid feedback. However, there are incomplete palpation landmarks for all the presented models, the tissue representation does not reflect the multiple puncture resistance forces, and there are no reconfiguration options to allow IM residents to practice on different sizes or thoracic wall thicknesses. The lung may be unrealistic, and the rib cage may be flat (Figure 6 (a) and (b)) or have limited curvature. However, a flat geometry configuration can be readily molded.

<i>Model & Maker</i>	<i>Image</i>	<i>Pros</i>	<i>Cons</i>	<i>Price (USD)</i>
THMT-30 SIMULAB [[37]]		<ul style="list-style-type: none"> -Portable -Multiple use -Fluid feedback -Ultrasound compatible 	<ul style="list-style-type: none"> -Unrealistic appearance -Incomplete palpation landmarks (no clavicle) -Poor tissue representation (single layer) -Non reconfigurable 	\$2,992

<p>Ultrasound-Guided Thoracentesis Simulator-Strap-On Set</p> <p>ERLER ZIMMER [[38]]</p>		<p>-Portable</p> <p>-Fluid feedback</p>	<p>-Incomplete palpation landmarks (no clavicle or scapula)</p> <p>-Non reconfigurable</p> <p>-Poor tissue representation (single layer)</p>	<p>\$4620</p>
<p>MW4: Ultrasound Guided Thoracentesis Simulator</p> <p>Kyoto Kagaku America Inc. [[22]]</p>		<p>-Ultrasound friendly</p> <p>-Realistic appearance</p> <p>-Fluid feedback</p>	<p>-Incomplete palpation landmarks (no clavicle or scapula)</p> <p>-Non reconfigurable</p> <p>-Poor tissue representation (single layer)</p>	<p>\$2900</p>

Table 1: Analysis of existing thoracentesis training mannequins.

As the aim of this research is to develop a reconfigurable design and fabrication solution for a thoracentesis training mannequin, an understanding of the key demographics requiring this procedure, and the degree of variability of the patient demographic needs to be evaluated to define the solution space.

2.2 Patient characteristics

In the United States, an estimated 178,000 thoracenteses are performed yearly. Mynarek et al. showed that the patient population distribution of their study, comprised of 711 performed thoracenteses, is skewed towards older adults; however, a notable percentage (19%) of cases between 0-9 years of age (Figure 7, in red) have been reported, and 22% are between 50-59 years old [[23]]. This younger population is particularly problematic; as juvenile patients are often less resilient than slightly older ones. Furthermore, this younger population is more likely to be anxious, and potentially more distressed, leading to a higher risk of complications due to shaking or flinching, so much so, that some patients require the administration of drugs to calm them down [[7]]. Despite this, the majority of mannequins are designed to simulate the average 30 year old male, representing only 8.2% of the thoracentesis patient population. (Figure 7, in green) [[23]].

In order to accurately simulate patients of all sexes and ages, sizing relationships are needed to correlate age and sex size metrics to the mannequin size. Weaver et al. used computed tomography (CT) scans and tracked rib cage landmarks in males to determine that there are distinct growth patterns: (1) a linear growth pattern from 6 months to 20 years, (2) a moderate size increase between 20 to 30 years, and (3) a quasi-plateau region for ages > 30 (Fig. 8) [[41]]. This finding is backed by Subit et al., who have determined that the growth of the rib cage between 0-20 years of age is linear, before slowing significantly upon maturation [[34]].

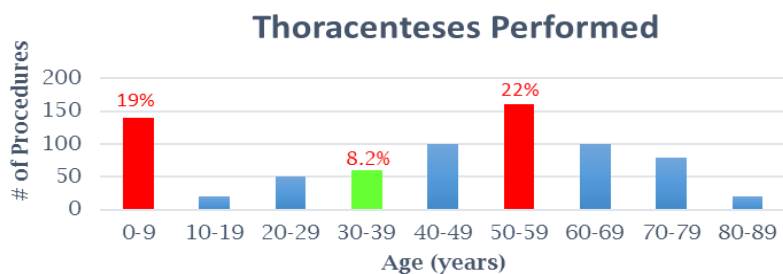


Figure 7: Age distribution of thoracentesis (adapted from Mynarek et al. [[23]]).

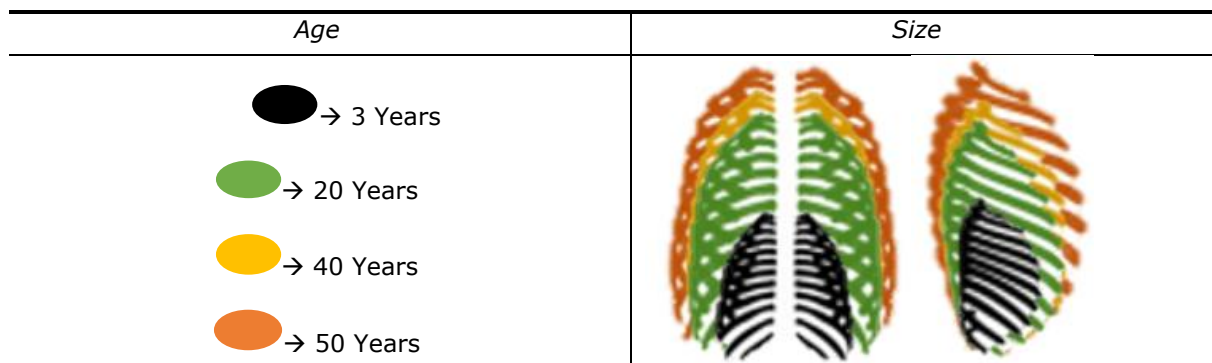


Figure 8: Rib cage growth from 3 years to 50 years of age (aligned by base) (adapted from Weaver et al. [[41]]).

For the clavicle, McGraw et al. analyzed digital chest radiographs from birth to 18 years of age for both males and females to determine its growth patterns. These results are presented in Fig. 9, where it can be seen that the growth pattern for females and males is slightly different, as this study indicates that females and males achieve 80% of their clavicle length by 9 and 12 years of age respectively [[21]]. However, for this research the growth of both clavicles may still be considered linear throughout this range, as shown by the high R^2 correlation value.

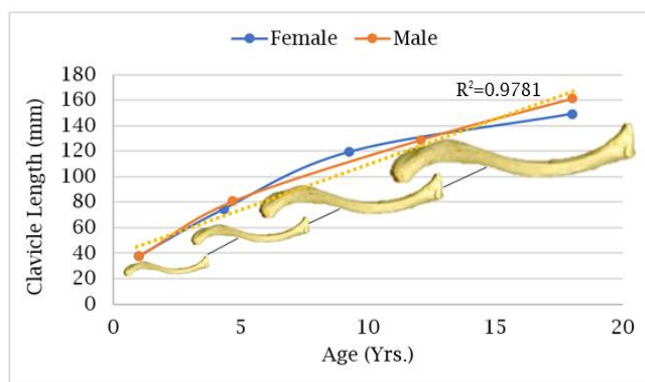


Figure 9: Growth of male vs. female clavicle from 0-18 years of age (adapted from McGraw et al. [[21]]).

No literature was found for the scapula growth patterns; however, assumptions related to its growth pattern can be made. By analyzing images such as Figure 10 [[8]], and with the knowledge that the rib cage and clavicle grow in a linear manner, it has been reasoned that since there are no additional bones or structures within the connection of the rib cage, clavicle, and scapula other than the acromio-clavicular joint and sterno-clavicular joint, that the scapula does as well. The scapula is a necessary palpation landmark; consequently, an understanding of its size is relevant.

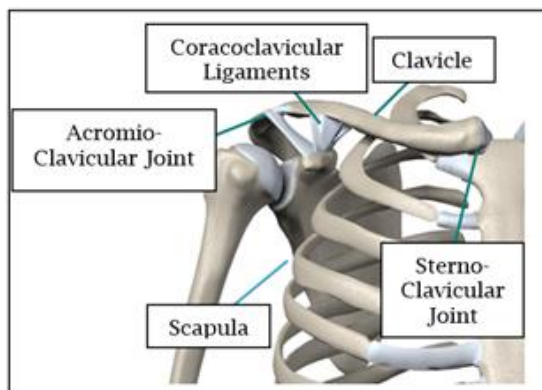


Figure 10: Chest girdle skeletal structure (adapted from [[8]]).

In addition to the age and size differentials for the thoracentesis patients, Harcke et al. have shown that the thoracic wall thickness varies greatly between individuals. In Figure 11(a), two extreme regions are highlighted. The thoracic wall thickness range varies from 3.07 cm to 9.35 cm [[12]]. Furthermore, in the United States, obesity rates are a serious concern. With more than 1/3 adults, and 1/6 children classified as overweight [[29]] (Figure 11(b)), the chest wall thickness, and “feel” during the puncture is highly variable, and this must be considered for this demographic as well. Jiang et al. [[15]], Poniatowski et al. [[29]], and Okamura et al. [[25]] have studied various effects of variables on soft tissue puncture forces, however no literature was found regarding the puncture forces of the thoracic wall specifically. Given the complexity of the thoracic wall (which consists of multiple layers, including skin, muscle, adipose tissue, and pleura), and the need for a highly realistic puncture resistance, an experimental procedure to determine the necessary forces was performed.

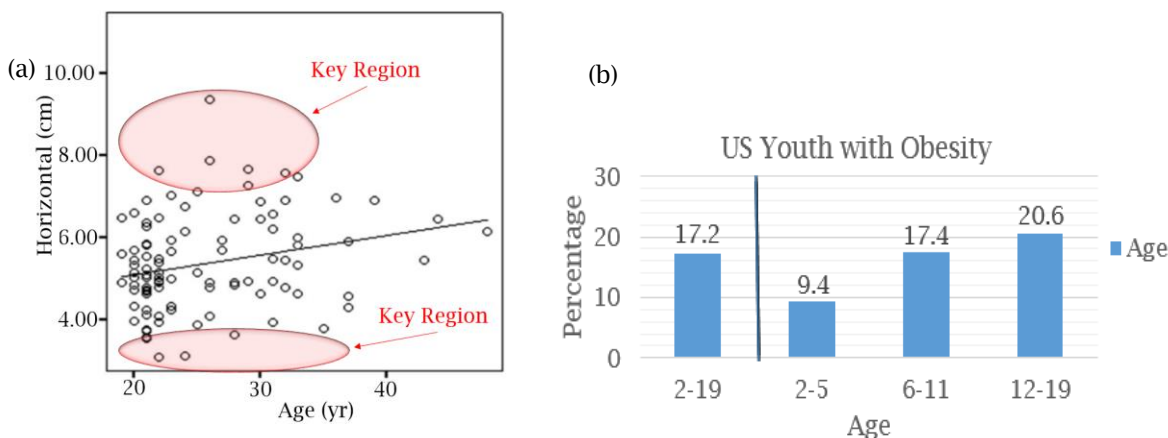


Figure 11: (a) Chest wall thickness variation with age (adapted from Harcke et al. [[12]]), (b) US youth obesity (adapted from [[29]]).

The lessons learned from the anatomy review are:

- The clavicle and rib cage grow linearly and uniformly up to 20 years of age, and it can be reasoned that the scapula does as well.
- There are no additional bones or structures within the connection of the rib cage, clavicle, and scapula (acromio-clavicular joint, sterno-clavicular joint excepted).
- A 20-year-old adult has a rib cage and clavicle approximately 4 times larger than a 1-year-old child, and 1.25 times larger than a 9-year-old child.

To improve upon the existing solutions, an ideal training mannequin would:

- Be anatomically accurate, and contain reference landmarks (scapula, clavicle, rib cage);
- Possess realistic tissues in terms of both depth, layers and 'feel' (resistant forces);
- Be reconfigurable to represent different sizes, ages, sexes;
- Be adaptable in terms of body constitutions (i.e. obesity);
- Be directly linked to the final manufacturing process (i.e. silicon molding)
- Contain a feedback mechanism (actual liquid removal); and
- Be self-resealing (for multiple uses)

Therefore, a CAD model solution needs to be developed to adjust to various scenarios, and linked to the mold core and cavity blocks, based on the demographic information.

2.3 CAD Strategies

Reconfigurable CAD models combined with Additive Manufacturing (AM) processes provide superior means to improve prototypes and products. When knowledge from the Medical and Kinesiology fields of study are incorporated into these processes, attractive solutions to bio-medical and bio-mechanical problems present themselves (Figure 1). The development of a superior thoracentesis training mannequin is a prime example of this. A summary of literature pertaining to CAD modelling and thoracentesis education and training is presented in Tab. 2 with categorical rankings. Low scores indicate gaps in the research, which must be filled in order to develop a superior mannequin. Based on the review of literature, it has been determined that there are gaps in the modelling of internal organs, the realism of resistive forces, the re-configurability/parametric design of models, and in the implementation of quick-change elements. This information, along with the anatomy lessons learned, influence the component CAD models.

<i>Aspect</i>	<i>Models Internal Organs</i>	<i>Contains Muscle / Tissues</i>	<i>Contains Ribcage and Skeletal Support</i>	<i>Interactive Model</i>	<i>Realistic resistive forces</i>	<i>Parametric / Reconfigurable Design</i>	<i>For Training</i>	<i>Quick Change / Adaptable</i>
<i>Source</i>								
5	0	5	5	2	0	1	5	0
40	0	3	5	5	3	0	5	0
11	0	5	4	5	3	0	5	0
18	5	4	5	1	0	1	1	0
27	5	4	5	1	0	0	3	0
24	5	3	4	2	0	0	3	0
17	0	0	5	3	5	0	4	0
12	3	4	5	5	4	0	5	0
4	0	5	3	0	5	0	0	0
Total	18/45	33/45	41/45	24/45	20/45	2/45	31/45	0/45

Table 2: Thoracentesis modeling summary.

2.4 Additive Manufacturing Processes

The AM process family deconstructs complex 3D shapes into a set of layers which contain boundary contours and fill regions. There are 7 main classifications of Additive Manufacturing, which are summarized in Tab. 3. The strengths and weaknesses, as well as manufacturing time and materials from each classification are analyzed to determine which best suits this application [[20]].

<i>Family</i>	<i>Strength</i>	<i>Weakness</i>	<i>Materials</i>	<i>Time</i>
Material extrusion (fused filament)	Complex structures with support	Lower accuracy, stair case surface finish, support material removal post processing required	Polymers, thermoplastics	Fast
Powder bed fusion	Integrated support structure (powder bed)	Size limitations, Expensive, support material removal post processing required	Metals, polymers	Slow
Material jetting	High accuracy	Limited material use	Polymers,	Moderate
Binder jetting	Wide range of materials	Need for post processing	Metals, ceramics, polymers	Fast
Directed energy deposition	High quality and strength	Limited materials (metals only), expensive	Metals	Moderate
Vat photopolymerization	High quality	Lengthy post-processing	Polymers, resins	Slow
Sheet lamination	High speed	Need post processing	Paper, polymers, sheet metals	Fast

Table 3: Summary of AM Processes.

Accuracy and a rough surface finish are secondary issues for this application, as representative anatomical components are encased in silicone. The model should be lightweight, yet have flexibility and strength. A full scale rib cage model is large. Consequently, a material extrusion AM process using ABS material [2] in a machine with a 400 x 350 x 400 build envelop (Fortus 400 [10]) is used for the fabrication of the anatomical components, and the inserts and molds.

3 METHODOLOGY

Building from previous research, a procedure was refined for the development of a thoracentesis mannequin using a methodology modified from Kalami et al. (Figure 12) [[16]]. The specific development of a medical device (in this case a training mannequin) is encompassed within the product development process, which includes identifying the specific market opportunity or need, assessing the current product offerings, determining the functional requirements and design constraints, creating a functional model, manufacturing the prototype, and testing and validating the design. The steps of creating the model to validating it are repeated as the model is refined and improved. This procedure is directly related to the theme presented in Figure 1, as it incorporates multiple disciplines to develop a superior solution.

With the functional requirements determined, the reverse engineering of human attributes and evaluation of design constraints was performed through an experimental cadaveric puncture

procedure. In this experiment, 5 participants performed 3 experimental punctures in 3 separate locations, each with different tissue characteristics (Figure 13(a), (b), (c)).

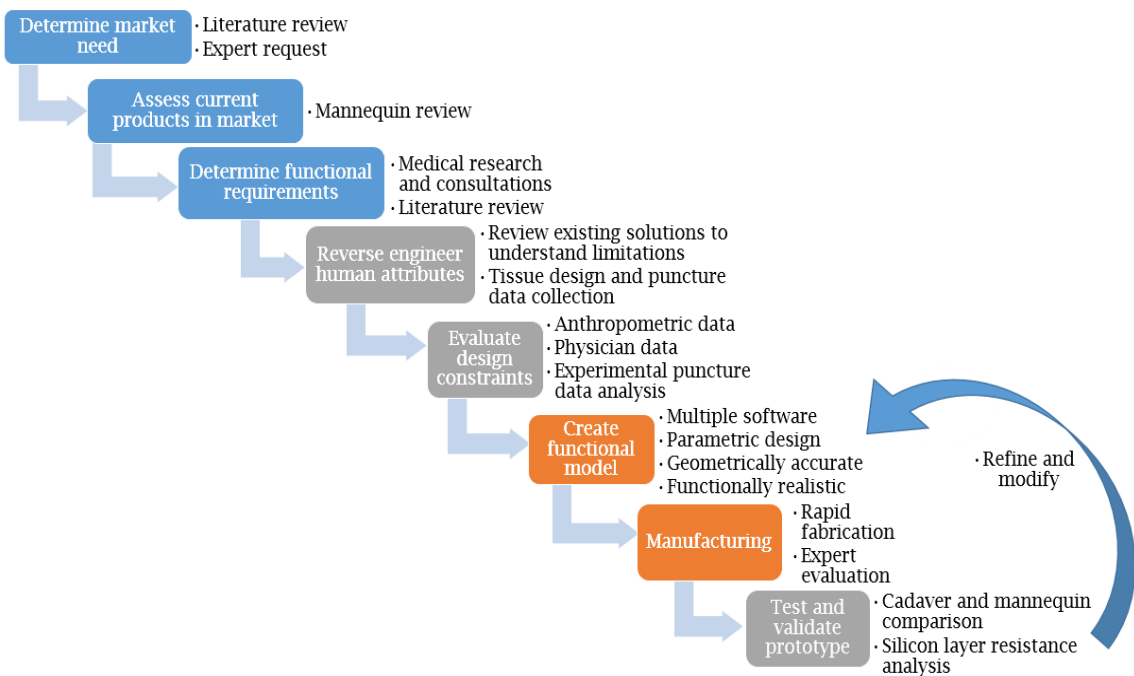


Figure 12: Methodology for medical prototype development modified from Kalami et al. [[16]].

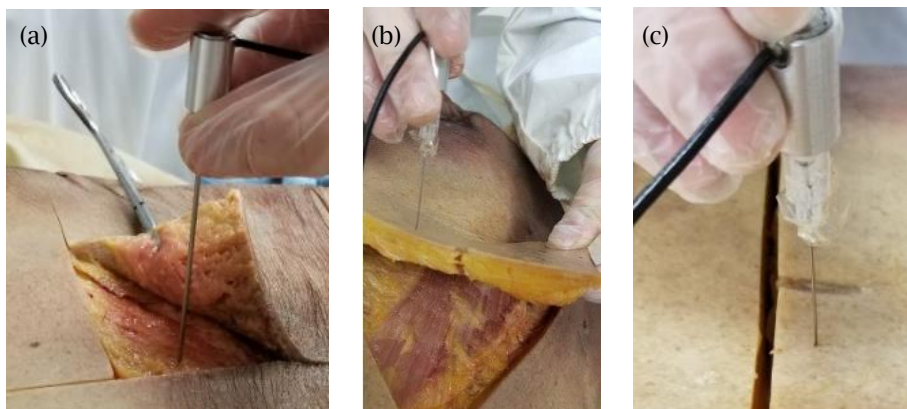


Figure 13: (a) Position 1 experimental cadaver puncture site, (b) Position 2 experimental cadaver puncture site, (c) Position 3 experimental cadaver puncture site.

A transducer-fitted thoracentesis needle was used along with a custom WIDACS (WIreless Data ACquisition System) [[13]] to measure peak forces, impulses, and pulse widths of each puncture. Along with the key variables aforementioned, a statistical investigation into the necessary layers for representing the human thoracic cross-section was performed. Punctures were then repeated on the

mannequin currently at use at the University of Windsor (Figure 6 (a) and (b)), and the results compared.

The force data were calibrated to Newtons and low-pass filtered using a 4th order Butterworth filter with a cut-off of 25 Hz (Figure 14). Data that contained a bias was adjusted manually by taking the absolute values, integrating them, and replotting them. Data outliers were removed, and replaced with filler points representative of the means of each position, and statistical analyses were performed to determine the relations between layers.

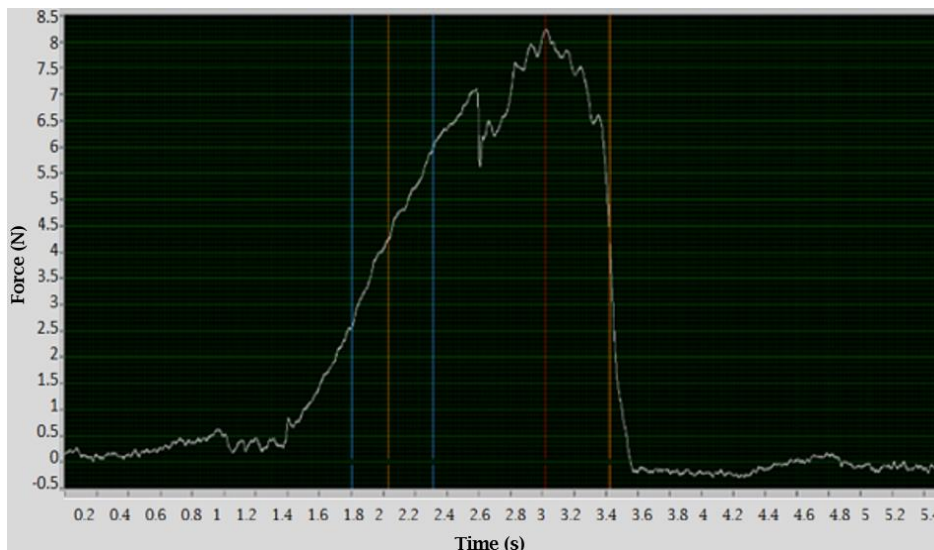


Figure 14: Cadaver puncture profile.

3.1. CAD Modelling

Open source models generated from Computed Tomography (CT) scans were obtained for the skeletal structures in order to optimize anatomical accuracy. These files were not in a suitable format to be readily modified in CAD software, so a procedure outlined in Figure 15 was followed. Through the manipulation and trimming of meshes, solid body CAD models were developed and assembled. Outer surfaces of the solid bodies appear triangulated due to the methods by which the triangulated shells were filled. From these CAD files, an artificial “tissue” model was generated through spline and lofting commands (Figure 16). In the development of this tissue, 6 planes were created, on which cross-sectional profiles were generated. The profiles were joined using lofting commands, which automatically generated lofting path lines, which resulted in a smooth outer tissue profile.

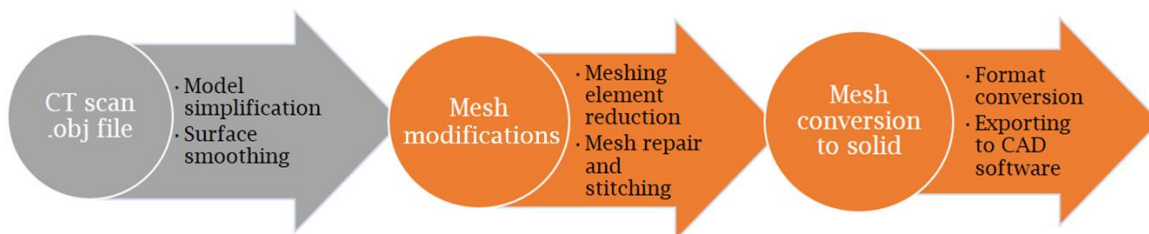


Figure 15: CT scan file conversion procedure.

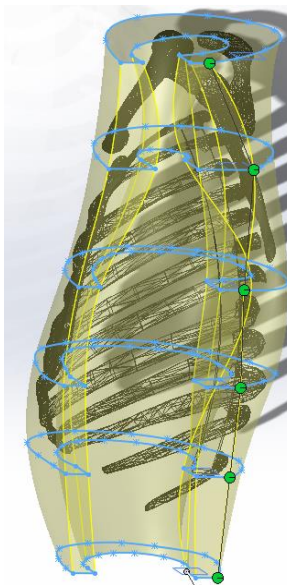


Figure 16: Spline and lofting techniques used to generate artificial tissue.

A scaling table for re-configuring the CAD skeletal structures to represent patients from 0-20 years of age (Tab. 4) is developed using the observed growth data. For patients older than this range, manual modifications may be made, as it has been stated that the growth of the skeletal structures involved is minimal [[21]], [[41]], [[34]].

Sex	Male				Female			
Age Group (years)	0-4	4-12	12-18	18-100	0-4	4-9	9-18	18-100
Length (mm)	37.61	80.65	129.03	161.29	37.8	74.58	119.33	149.16
% of growth	23.32	50	80	100	25.34	50	80	100
Scaling Input	0.416	0.892	1.427	1.784	0.420	0.829	1.326	1.657

Table 4: Scaling factor inputs.

With the scaling factors established, a 3 component overmold package was designed for the artificial tissue to be molded around the skeletal elements. Parametric relationships were implemented such that the tissue could be easily modified to represent a different body composition, resulting in an automatically modified mold (Figure 17 and Figure 18).

The completed models were built using a 0.254 mm slice height, ABS-M30 [[2]] build material, and SR-30 as the support material [[33]], as it is dissolvable in a caustic bath (allowing for internal supports, and easy removal of this support material afterwards). A variable-hardness silicone was selected for use [[39]] based on the market review, which showed that all existing training mannequins contained silicone to represent the human tissue. With this silicone, as well as a modifiable skeletal structure and a parametric mold, an alpha prototype was developed.

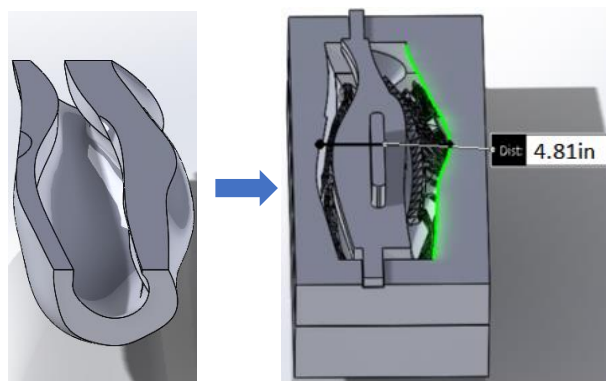


Figure 17: Initial mold obesity configuration.

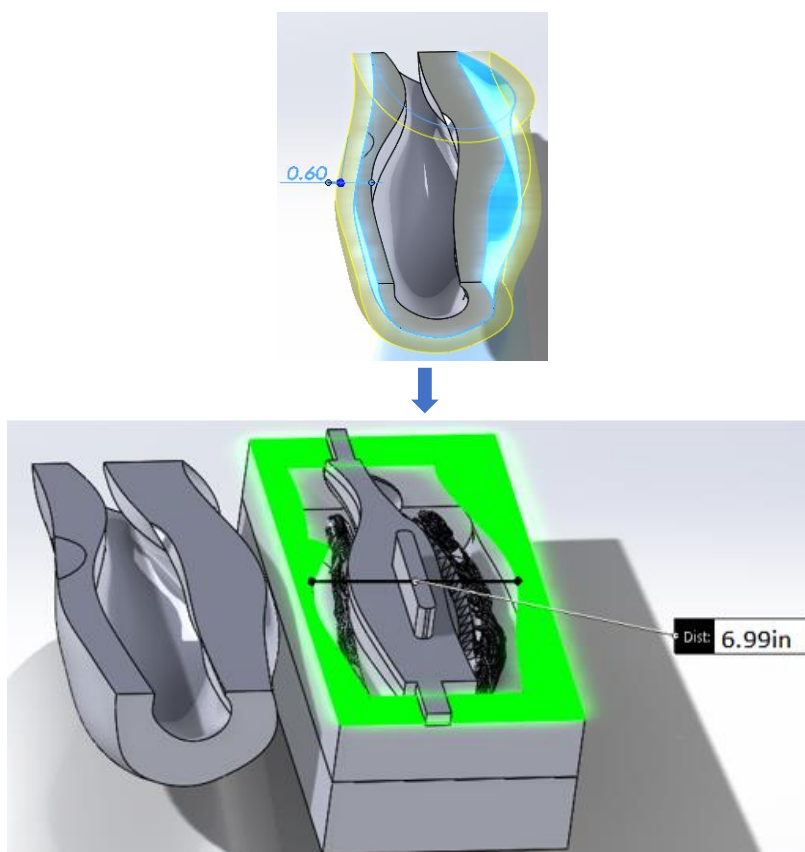


Figure 18: Parametric obesity adaptation of overmold elements.

In order to refine tissues, the alpha prototype may be analyzed using the same experimental procedure outlined above, comparing the individual layers, as well as the overall tissue, to the cadaveric punctures in order to determine the source(s) of error, if any.

4 RESULTS

Manual puncture curve processing and integration yielded mean representative curves for the peak force and impulse of the cadaver punctures, as well as the mannequin punctures (Figure 19). The statistical means and standard deviations for the peak force, impulse, and pulse width from the cadaver and mannequin punctures are summarized in Table 5. From these results, it has been determined that the mannequin currently in use at the University of Windsor does not provide accurate resistive forces.

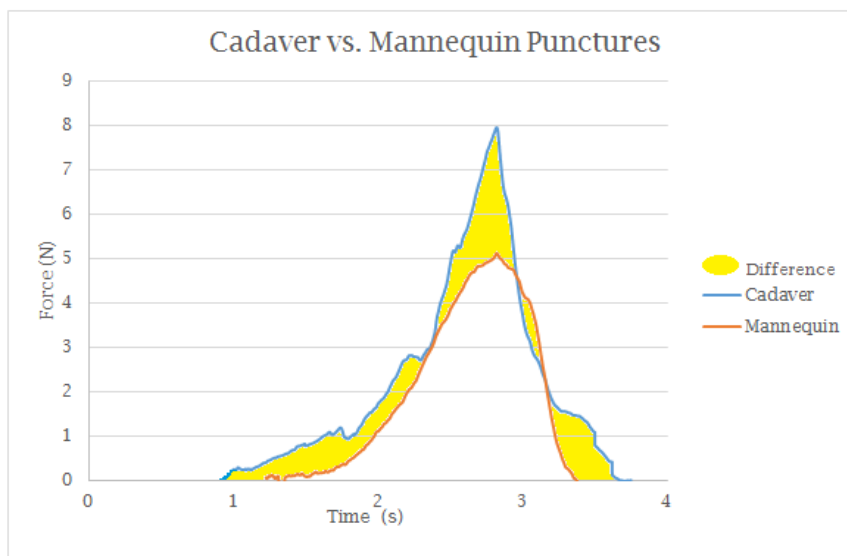


Figure 19: Manually processed mean cadaver and mannequin puncture curves.

	<i>Peak Force (N)</i>	<i>SD (N)</i>	<i>Impulse (N·S)</i>	<i>SD (N·S)</i>	<i>Pulse Width (S)</i>	<i>SD (S)</i>
Cadaver	7.229	3.508	5.361	3.030	0.514	0.230
Mannequin	5.169	0.082	4.355	0.096	0.856	0.013
% Difference	28.495		18.769		-66.667	

Table 5: Cadaver and mannequin puncture means.

A 5X3 Repeated Measures ANOVAs (ANalysis Of VAriance) revealed a main effect of position across all three criteria. Through further analysis of output data, it was determined that position 2 was statistically similar to position 3. Based on this, the entire thoracic cross section (represented in position 3), can be statistically represented by position 2 (skin and adipose tissue).

With target values from Tab. 5 the statistical results indicating a 2-layer solution for tissue resistant forces is appropriate, the anatomical and process related CAD models, and the AM FDM process, the production of multiple prototypes for the skeletal (Figure 20(a)) and overmolding components (Figure 20(b)) variants is realized with minimal effort. Silicon layers, to emulate the resistance observed in the cadaveric puncture data, were then poured into the mold and a dual-layer alpha prototype with necessary landmarks to the palpation sequence, with variable wall thickness, was fabricated (Figure 21(a), (b) and (c)). By using procedures outlined in the experimental testing, individual layers, as well as the entire cross section may be analyzed in order to refine the puncture force resistances.

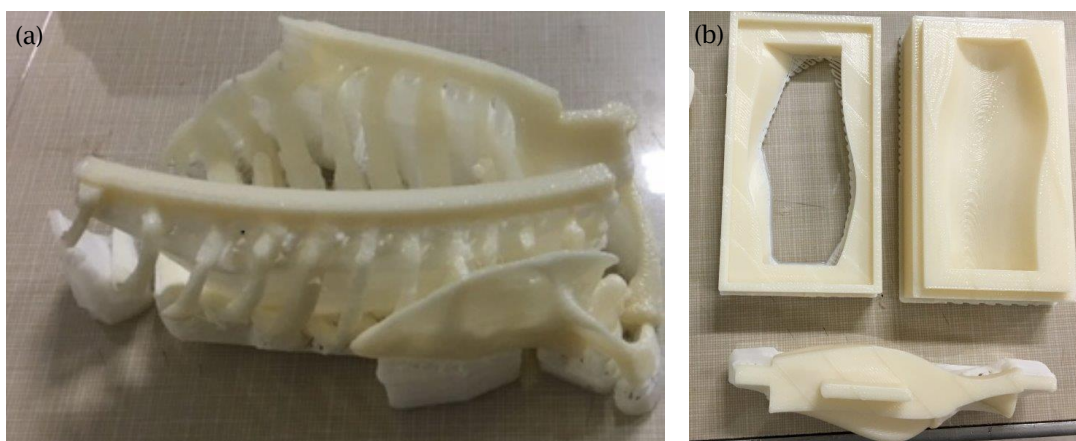


Figure 20: (a) Reconfigurable skeletal prototype elements, (b) Parametric overmold components.

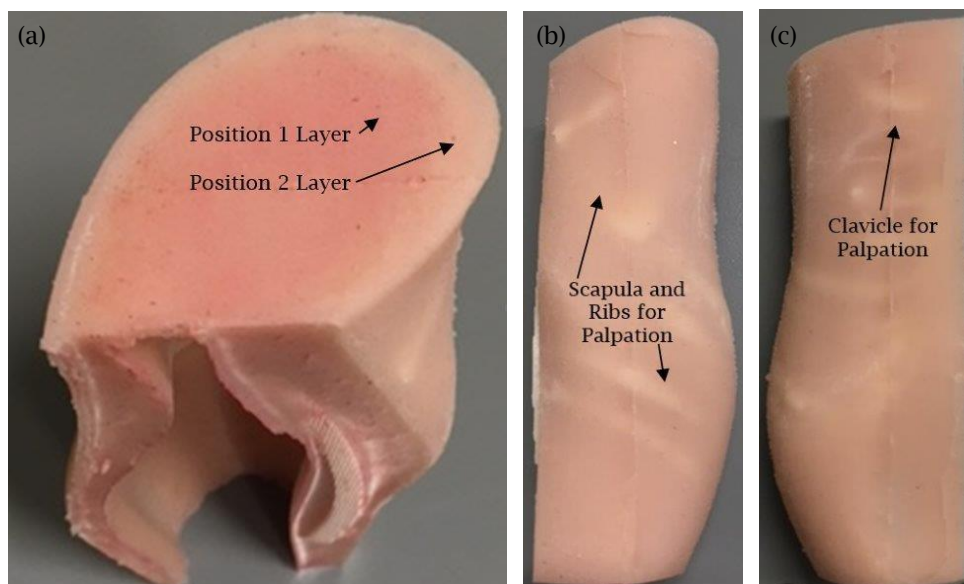


Figure 21: Reconfigurable dual-layer alpha prototype.

5 SUMMARY, CONCLUSIONS AND FUTURE WORK

5.1. Future Work

A 'quick change' system for altering the tissue thickness locally in the puncture region has been designed and needs to be tested. To advance this research, and the mannequin design further, a realistic lung and feedback mechanism will be developed. A frame to house the assembly, as well as a circuit-based notification system to indicate procedural error may be implemented. This system would consist of an open circuit layer covering the internal organs, which would be completed upon contact with the metallic needle, triggering a signal to notify the user of organ contact. Lastly,

several iterations of the model will be developed, and tested by a larger group of medical professionals to refine the prototype.

5.2. Summary and Conclusions

From the medical literature, it was determined that conventional teaching methodologies were inadequate, with 40% of emergency physicians tested being unable to identify key landmarks for an optimal puncture on test subjects [[9]]. Through the implementation of a thoracentesis training mannequin, written and clinical performance scores of students increased by 71% [[40]]. However, for a thoracentesis procedure, a high percentage of patients are between 0–9 years old, and there is a high likelihood of the potential patient being obese. Existing training mannequins do not reflect these patient variations. The development of parametric CAD models, combined with flexible manufacturing solutions, allow for reconfigurations for both the patient and fabrication mold models. The strategies implemented in this research are applicable to a wide array of applications in the medical training mannequin domain. Better models and simulations of different types of patients better prepares medical personnel to handle varying real life cases. This has the potential to improve thoracentesis procedures and reduce errors. These design and manufacturing techniques can provide the opportunity for other innovative solutions for current medical training.

6 ACKNOWLEDGEMENTS

This research is partially funded by the NSERC Discovery Grant. Special thanks to Dr. Joel Cort, Mr. Donald Clarke, Besim Kalajdzic, Lakshmi Kamala, Sarah Zhang and Yunfei Teng for their support.

Andre Khayat, <http://orcid.org/0000-0002-9243-1929>

R. Jill Urbanic, <http://orcid.org/0000-0002-2906-7618>

Anna Farias, <http://orcid.org/0000-0001-7508-6329>

Beth-Anne Schuelke-Leech, <http://orcid.org/0000-0003-0503-830X>

7 REFERENCES

- [1] 3DEO: Costs of Traditional vs. Additive Manufacturing, Gardena, CA, 2017, <https://news.3deo.co/strategy/costs-traditional-vs-additive-manufacturing>.
- [2] ABS M-30, <http://www.stratasys.com/materials/search/abs-m30>, Stratasys.
- [3] Arrow-Clarke Pleura-Seal Thoracentesis Kits, <http://www.medline.com/product/Arrow-Clarke-Pleura-Seal-Thoracentesis-Kits-by-Teleflex/Thoracentesis-Trays/Z05PF33639?question=&index=P3&indexCount=3>, Teleflex.
- [4] Berg, D.; Bergm K.; Riesenber, L. A.; Weber, D.; King, D.; Mealer, K.; Justice, E. M.; Geffe, K.; Tinkoff, G.: The Development of a Validated Checklist for Thoracentesis, *American Journal of Medical Quality*, 28(3) 2013, 220-226. <https://doi.org/10.1177/1062860612459881>.
- [5] Bernman, N. B.; Durning, S. J.; Fischer, M. R.; Huwendiek, S.; Triola, M. M.: The Role for Virtual Patients in the Future of Medical Education., *Academic Medicine*: September 2016, 91(9) 2016, 1217-1222. <https://doi.org/10.1097/ACM.0000000000001146>
- [6] Brauner, M. E.; Bailey, R. A.: Thoracentesis, *Medscape*, 2018, <https://emedicine.medscape.com/article/80640-overview#a9>.
- [7] Chandrasekhar, A. J.; Garrity, E.: Thoracentesis and Fluid Analysis, Loyola University, Chicago, IL, 2006, www.lumen.luc.edu/lumen/MedEd/medicine/pulmonar/procedur/thorac_f.html.
- [8] Chest Girdle Skeletal Structure, <https://www.visiblebody.com/blog/3d-skeletal-system-bones-of-the-thoracic-cage>, VISIBLE BODY.
- [9] Ferrie, E. P.; Collum, N.; McGovern, S.: The right place in the right space? Awareness of site for needle thoracocentesis, *Emergency Medicine Journal*, 22(11), 2005, 788-789. <https://doi.org/10.1136/emj.2004.015107>.

- [10] Fortus 400 Mc, <http://www.stratasys.com/resources/search/white-papers/fortus-360mc-400mc?resources=58ebc939-4384-4476-95c0-63055c5ee9af>, Stratasys.
- [11] Guanchao, J.; Hong, C.; Shan, W.; Qinghuan, Z.; Xiao, L.; Kezhong, C.; Xizhao, S.: Learning curves and long-term outcome of simulation-based thoracentesis training for medical students, *BMC Medical Education*, 11(39) 2011. <https://www.ncbi.nlm.nih.gov/pubmed/21696584>
- [12] Harcke, H. T.; Pearse, L. A.; Levy, A. D.; Getz, J. M.; Robinson, S. R.: Chest Wall Thickness in Military Personnel: Implications for Needle Thoracentesis in Tension Pneumothorax, *Military Medicine*, 172(12), 2007, 1260–1263. <https://doi.org/10.7205/MILMED.172.12.1260>.
- [13] Custom WIDAQS, <http://www.uwindsor.ca/kinesiology/482/dr-joel-cort>, Cort Research and Innovation Inc.
- [14] Huang, G. C. et al.: Beyond the Comfort Zone: Residents Assess Their Comfort Performing Inpatient Medical Procedures, *The American Journal of Medicine*, 119(1), 2006, 17–24. <https://doi.org/10.1016/j.amjmed.2005.08.007>.
- [15] Jiang, S.; Li, P.; Yu, Y.; Liu, J.; Yang, Z.: Experimental study of needle-tissue interaction forces: effect of needle geometries, insertion methods and tissue characteristics, *Journal of biomechanics*, 47(13) 2014, 2244–3353. <https://doi.org/10.1016/j.jbiomech.2014.08.007>.
- [16] Kalami, H.; Khayat, A.; Urbanic, R. J.: Investigating 'Exo-Skeleton' Design and Fabrication Challenges for the Hand Region Using Material Extrusion Processes, *IFAC-PapersOnLine*, 49(31), 2016, 30–35. <https://doi.org/10.1016/j.ifacol.2016.12.157>.
- [17] Katballe, N.; Moeller, L. B.; Olesen, W. H.; Litzner, M. M.; Andersen, G.; Nekrasas, V.; Licht, P. B.; Bach, P.; Pilegaard, H. K.: A Novel Device for Accurate Chest Tube Insertion: A Randomized Controlled Trial, *The Annals of Thoracic Surgery*, 101(2), 2016, 527–532. <https://doi.org/10.1016/j.athoracsur.2015.07.017>.
- [18] Kaye, J.; Metaxas, D. N.; Primiano Jr., F. P.: A 3D Virtual Environment for Modeling Mechanical Cardiopulmonary Interactions, *CVRMed-MRCAS'97, Lecture Notes in Computer Science*, 1205, 1997.
- [19] Lechtzin, N.: How to Do Thoracentesis, Johns Hopkins University School of Medicine, 2016, <https://www.merckmanuals.com/en-ca/professional/pulmonary-disorders/diagnostic-and-therapeutic-pulmonary-procedures/how-to-do-thoracentesis>.
- [20] Loughborough University, About Additive Manufacturing, Leicestershire, UK, <http://www.lboro.ac.uk/research/amrg/about/the7categoriesofadditivemanufacturing/>.
- [21] McGraw, M. A.; Mehlman, C. T.; Lindsell, C. J.; Kirby, C. L.: Postnatal Growth of the Clavicle: Birth to Eighteen Years of Age, *Journal of Pediatric Orthopedics*, 29(8), 2009, 937–943. <https://doi.org/10.1097/BPO.0b013e3181c11992>.
- [22] MW4: Ultrasound Guided Thoracentesis Simulator, https://www.kkamerica-inc.com/mw4_ultrasound_guided_thoracentesis_simulator/, Kyoto Kagaku America Inc.
- [23] Mynarek, G.; Brabrand, K.; Jakobsen, J. A.; Kolbenstvedt, A.: Complications Following Ultrasound-Guided Thoracocentesis, *Acta Radiologica*, 45(5), 2004, 519–522. <https://doi.org/10.1080/02841850410005804>.
- [24] Ngo, C.; Schlözer, R.; Vollmer, T.; Winter, S.; Misgeld, B.; Leonhardt, S.: A simulative model approach of cardiopulmonary interaction, *IFMBE Proceedings*, 51, 2015, 1679–1682. https://doi.org/10.1007/978-3-319-19387-8_408
- [25] Okamura, A. M.; Simone, C.; O'Leary, M. D.: Force modeling for needle insertion into soft tissue, *IEEE Transactions on Biomedical Engineering*, 51(10), 2004, 1707–1716. <https://doi.org/10.1109/TBME.2004.831542>.
- [26] Overweight & Obesity Statistics, National Institute of Diabetes and Digestive and Kidney Diseases, U.S. Department of Health and Human Services, Bethesda, MD, 2017, www.niddk.nih.gov/health-information/health-statistics/overweight-obesity.
- [27] Penjweini, R.; Kim, M. M.; Dimofte, A.; Finlay, J. C.; Zhu, T. C.: Deformable medical image registration of pleural cavity for photodynamic therapy by using finite-element based method, *Proceedings of SPIE--the International Society for Optical Engineering*, 2016. <https://doi.org/10.1117/12.2211110>.

- [28] Pleural Effusion Graphic, <http://geoface.info/ef8714/anatomy-and-physiology-of-pleural-effusion>, GEOFACE.
- [29] Poniatowski, L. H.; Somani, S. S.; Veneziano D.; McAdams, S.; Sweet, R. M.: Characterizing and Simulating Needle Insertion Forces for Percutaneous Renal Access, *Journal of Endoutology*, 30(10), 2016, 1049–1055. <https://doi.org/10.1089/end.2016.0342>.
- [30] Prestridge, A.: *Thoracentesis, Current Procedures, Pediatrics*, McGraw-Hill Education, 2007, <https://accesspediatrics.mhmedical.com/content.aspx?bookid=444§ionid=40089969>.
- [31] Simel, D. L.: *Make the Diagnosis: Thoracentesis, The Rational Clinical Examination: Evidence-Based Clinical Diagnosis*, McGraw-Hill Education, 2009, <http://jamaevidence.mhmedical.com/content.aspx?bookid=845§ionid=75186098>.
- [32] Slic3r, <http://slic3r.org>, Ranellucci, A.; Lenox, J.
- [33] SR-30, <http://investors.stratasys.com/news-releases/news-release-details/new-fortus-support-material-helps-make-fdm-prototypes-and>, Stratasys.
- [34] Subit, D.; Sandoz, B.; Choisne, J.; Amabile, C.; Vergari, C.; Skalli, W.; Laporte, S.: Rib length variation with age and sex - Measurements from high-resolution low-radiation X-ray images of volunteer subjects, 4th International Technical Conference on the Enhanced Safety of Vehicles (ESV): Traffic Safety Through Integrated Technologies, Gothenburg, Sweden, 2015. <https://www-esv.nhtsa.dot.gov/Proceedings/24/files/24ESV-000313.PDF>.
- [35] Thoracentesis, Canadian Cancer Society, Toronto, ON, 2018, <http://www.cancer.ca/en/cancer-information/diagnosis-and-treatment/tests-and-procedures/thoracentesis/?region=on>.
- [36] Thoracentesis, The Johns Hopkins University, The Johns Hopkins Hospital, and Johns Hopkins Health System, Baltimore, MD, 2018, https://www.hopkinsmedicine.org/healthlibrary/test_procedures/pulmonary/thoracentesis_92,P07761.
- [37] Ultrasound Thoracentesis Model THM-30, <https://www.simulab.com/products/ultrasound-thoracentesis-model>, SIMULAB.
- [38] ULTRASOUND-GUIDED THORACENTESIS SIMULATOR - STRAP-ON SET, <https://www.erlerzimmer.de/shop/en/medical-simulators/ultrasound/10075/ultrasound-guided-thoracentesis-simulator-strap-on-set>, ERLER ZIMMER.
- [39] Variable Hardness Silicon, <http://www.liquidsilicone.net/product/list-155-en.html>, DONGGUAN GUOCHUANG SILICONE CO., LTD.
- [40] Wayne, B.; Barsuk, J.; O'Leary, K.; Fudala, J.; MCGAGHIE, W.: Mastery Learning of Thoracentesis Skills by Internal Medicine Residents Using Simulation Technology and Deliberate Practice, *Journal of Hospital Medicine*, 3(1), 2008, 48-54. <https://doi.org/10.1002/jhm.268>.
- [41] Weaver, A. A.; Schoell, S. L.; Stitzel, J. D.: Morphometric Analysis of Variation in the Ribs with Age and Sex, *Journal of Anatomy*, 225(2), 2014, 246–261. <https://doi.org/10.1111/joa.12203>.
- [42] Wohlers, T. T.: *Additive Manufacturing and 3d Printing State of the Industry: Annual Worldwide Progress Report*, Wohlers report 2015, Fort Collins, CO, 2015. <http://www.worldcat.org/title/wohlers-report-2015-3d-printing-and-additive-manufacturing-state-of-the-industry-annual-worldwide-progress-report/oclc/908262396>.